Z. angew. Math. Phys. 54 (2003) 532–550
0044-2275/03/030532-19
DOI 10.1007/s00033-003-1070-7

Zeitschrift für angewandte Mathematik und Physik ZAMP

Peristaltic transport of a Newtonian fluid in an asymmetric channel

Manoranjan Mishra and Adabala Ramachandra Rao

Abstract. Peristaltic transport of an incompressible viscous fluid in an asymmetric channel is studied under long-wavelength and low-Reynolds number assumptions. The channel asymmetry is produced by choosing the peristaltic wave train on the walls to have different amplitudes and phase. The flow is investigated in a wave frame of reference moving with velocity of the wave. The effects of phase difference, varying channel width and wave amplitudes on the pumping characteristics, streamline pattern, trapping, and reflux phenomena are investigated. The limits on the time averaged flux for trapping and reflux are obtained. It is observed that the pumping against pressure rise, trapping and reflux layer exists only when cross-section of the channel varies. The peristaltic waves on the walls with same amplitude propagating in phase produce zero flux rate as the channel cross-section remains same through out. The trapping and reflux regions increase as the channel becomes more and more symmetric and the maximum occurs for the symmetric channel.

Mathematics Subject Classification (2000). 76Z05, 92C35.

Keywords. Peristaltic transport, asymmetric channel, pumping, trapping, reflux.

1. Introduction

Peristaltic transport is a form of fluid transport generated by a progressive wave of area contraction or expansion along the length of a distensible tube containing fluid. Peristalsis is an inherent property of many biological systems having smooth muscle tubes which transports biofluids by its propulsive movements and is found in the transport of urine from kidney to the bladder, the movement of chyme in the gastro-intestinal tract, intra-uterine fluid motion, vasomotion of the small blood vessels and in many other glandular ducts. The mechanism of peristaltic transport has been exploited for industrial applications like sanitary fluid transport, blood pumps in heart lung machine and transport of corrosive fluids where the contact of the fluid with the machinery parts is prohibited.

Eventhough peristalsis existed very well in physiology, its relevance came about mainly through the works of Kill [6] and Boyarsky [1]. Later several mathematical and experimental models have been developed to understand the fluid mechanical

aspects of peristaltic motion. The mathematical models obtained by a train of periodic sinusoidal waves in an infinitely long two-dimensional symmetric channel or axisymmetric tubes containing a Newtonian or non-Newtonian fluid have been investigated by Shapiro *et al.* [9], Fung and Yih [5], Yin and Fung [14] , Shukla and Gupta [10], Srivastava and Srivastava [11], and many others. Many of these models explain the basic fluid mechanics aspects of peristalsis, namely the characteristics of pumping, trapping and reflux. These models are developed in two ways, one by restricting to small peristaltic wave amplitude with arbitrary Reynolds number and the other by lubrication theory in which the fluid inertia and wall curvature are neglected without any restriction of wave amplitude. The problems are investigated either in a fixed frame of reference or in a wave frame of reference moving with constant velocity of the wave simplifying the study to a case with stationary wavy walls. The accuracy of these models has been investigated numerically and experimentally by Takabatake and Ayukawa [12], Weinberg *et al.* [13], Yin and Fung [15] and several others.

Recently, physiologists observed that the intra-uterine fluid flow due to myometrial contractions is peristaltic-type motion and the myometrial contractions may occur in both symmetric and asymmetric directions, De Vries *et al.* [2].

Eytan *et al.* [4] have observed that the characterization of Non-pregnant woman uterine contractions is very complicated as they are composed of variable amplitudes, a range of frequencies and different wavelengths. It was observed that the width of the sagittal cross-section of the uterine cavity increases towards the fundus and the cavity is not fully occluded during the contractions. Recently Eytan and Elad [3] have developed a mathematical model of wall-induced peristaltic fluid flow in a two-dimensional channel with wave trains having a phase difference moving independently on the upper and lower walls to simulate intra-uterine fluid motion in a sagittal cross-section of the uterus. They have obtained a time dependent flow solution in a fixed frame by using lubrication approach. These results have been used to evaluate fluid flow pattern in a non-pregnant uterus. They have also calculated the possible particle trajectories to understand the transport of embryo before it gets implanted at the uterine wall. On the other hand a numerical technique using boundary integral method has been developed by Pozrikidis [7] to investigate peristaltic transport in an asymmetric channel under Stokes flow conditions to understand the fluid dynamics involved. He has studied the streamline patterns and mean flow rate due to different amplitudes and phases of the wall deformation. The existence of trapping region adjacent to the walls is also observed for some flow rates.

The aim of the present study is to investigate fluid mechanics effects of peristaltic transport in a two-dimensional asymmetric channel under the assumptions of long wavelength and low Reynolds number in a waveframe of reference which is different from the methods used by Pozrikidis [7] and Eytan and Elad [3]. The channel asymmetry is produced by choosing the peristaltic wave train on the walls to have different amplitude and phase due to the variation of channel width, wave

amplitudes and phase differences. In addition to reproducing the earlier results, we clearly bring out the significant effects on the pumping characterstics, trapping and reflux.

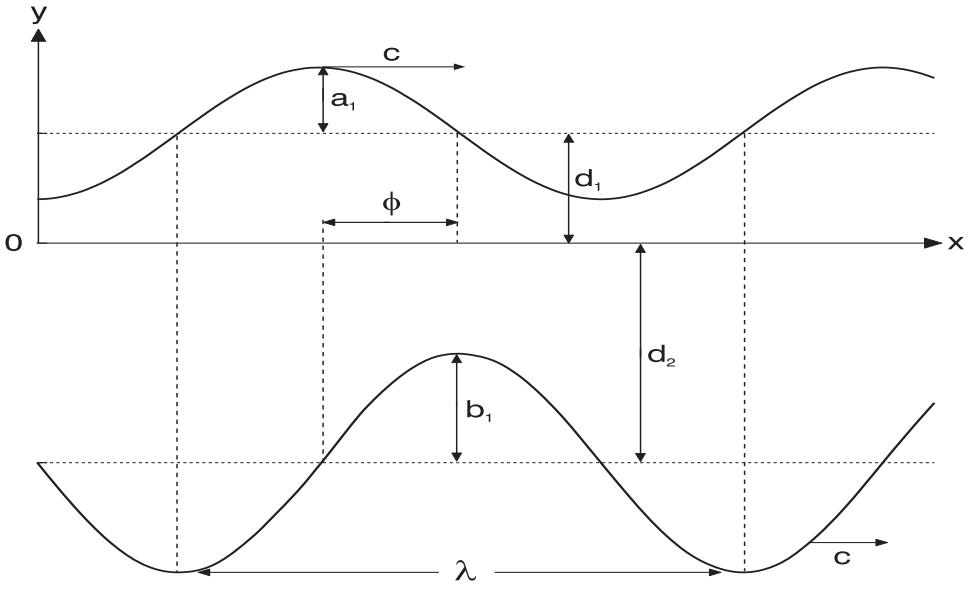

Figure 1. Schematic diagram of a two-dimensional asymmetric channel.

2. Mathematical formulation and solution

We consider the motion of an incompressible viscous fluid in a two-dimensional channel (see Fig. 1) induced by sinusoidal wave trains propagating with constant speed c along the channel walls

$$\begin{aligned} Y = H_1 &= d_1 + a_1 \cos \tfrac{2\pi}{\lambda}(X - ct), && \ldots\ldots \text{upper wall} \\ Y = H_2 &= -d_2 - b_1 \cos\big(\tfrac{2\pi}{\lambda}(X - ct) + \phi\big) && \ldots\ldots \text{lower wall,} \end{aligned} \tag{1}$$

where $a_1,\ b_1$ are the amplitudes of the waves, λ is the wave length, $d_1 + d_2$ is the width of the chanel, the phase difference ϕ varies in the range $0 \le \phi \le \pi$, $\phi = 0$ corresponds to symmetric channel with waves out of phase and $\phi = \pi$ the waves are in phase, and further a_1, b_1, d_1, d_2 and ϕ satisfies the condition $a_1^2 + b_1^2 + 2a_1 b_1 \cos\phi \le (d_1 + d_2)^2$.

Introducing a wave frame (x, y) moving with velocity c away from the fixed frame (X, Y) by the transformation

$$x = X - ct, \quad y = Y, \quad u = U - c, \quad v = V, \quad \text{and} \quad p(x) = P(X, t), \tag{2}$$

where (u, v) and (U, V) are velocity components, p and P are pressures in wave and fixed frame of references respectively. The pressure p remains a constant across any axial station of the channel under the assumption that the wave length is large and the curvature effects are negligible. Using the following non-dimensional variables:

$$\bar{x} = \frac{x}{\lambda}, \quad \bar{y} = \frac{y}{d_1}, \quad \bar{u} = \frac{U}{c}, \quad \bar{v} = \frac{V}{c\delta}, \quad \delta = \frac{d_1}{\lambda}, \quad \bar{p} = \frac{d_1^2 p}{\mu c \lambda}, \quad \bar{t} = \frac{ct}{\lambda}$$

$$h_1 = \frac{H_1}{d_1}, \quad h_2 = \frac{H_2}{d_1}, \quad d = \frac{d_2}{d_1}, \quad a = \frac{a_1}{d_1} \quad b = \frac{b_1}{d_1}, \quad R = \frac{cd_1}{\nu}, \quad \bar{\psi} = \frac{\psi}{d_1 c}$$

in the Navier-Stokes equations and eliminating pressure by cross differentiation, the equation for the flow in terms of stream function ψ, (dropping the bars, $u = \frac{\partial \psi}{\partial y}$, $v = -\frac{\partial \psi}{\partial x}$) is given by

$$R\delta\Big\{\psi_y\psi_{yyx} - \psi_x\psi_{yyy} + \delta^2(\psi_y\psi_{xxx} - \psi_x\psi_{xxy})\Big\} = \psi_{yyyy} + 2\delta^2\psi_{xxyy} + \delta^4\psi_{xxxx}, \quad (3)$$

here and in what follows subscripts x and y denote parial differentiations with respect to that variables.

The corresponding boundary conditions are

$$\left.\begin{array}{lll} \psi = q/2 & \text{at} & y = h_1 = 1 + a\cos 2\pi x \\ \psi = -q/2 & \text{at} & y = h_2 = -d - b\cos(2\pi x + \phi) \\ \frac{\partial \psi}{\partial y} = -1 & \text{at} & y = h_1 \quad \text{and} \quad y = h_2, \end{array}\right\} \quad (4)$$

where q is the flux in the wave frame and a, b, ϕ and d satisfy the relation

$$a^2 + b^2 + 2ab\cos\phi \le (1 + d)^2. \quad (5)$$

Under the assumptions of long wavelength $\delta << 1$ and low Reynolds number, the equation (3) becomes

$$\psi_{yyyy} = 0. \quad (6)$$

The solution of (6) satisfying the corresponding boundary conditions (4) is

$$\begin{aligned} \psi &= \frac{q + h_1 - h_2}{(h_2 - h_1)^3}\left(2y^3 - 3(h_1 + h_2)y^2 + 6h_1h_2y\right) - y \\ &\quad + \frac{1}{(h_2 - h_1)^3}\left((\frac{q}{2} + h_1)(h_2^3 - 3h_1h_2^2) - (h_2 - \frac{q}{2})(h_1^3 - 3h_2h_1^2)\right), \end{aligned} \quad (7)$$

where $h_2 \le y \le h_1$. The flux at any axial station in the fixed frame is

$$Q = \int_{h_2}^{h_1}(u + 1)dy = \int_{h_2}^{h_1} u dy + \int_{h_2}^{h_1} dy = q + (h_1 - h_2).$$

The average volume flow rate over one period $(T = \frac{\lambda}{c})$ of the peristaltic wave is defined as

$$\bar{Q} = \frac{1}{T}\int_0^T Q dt = \frac{1}{T}\int_0^T (q + (h_1 - h_2))dt = q + 1 + d. \quad (8)$$

The pressure gradient is obtained from the dimensionless momentum equation for the axial velocity $dp/dx = \psi_{yyy}$ and substituting for ψ from (6), we get

$$\frac{dp}{dx} = -12\left(\frac{1}{(h_1 - h_2)^2} + \frac{q}{(h_1 - h_2)^3}\right). \tag{9}$$

Integrating (9) over a tube length L, we get

$$\Delta p_L = p_L - p_0 = -12\left(\int_0^L \frac{dx}{(h_1 - h_2)^2} + q\int_0^L \frac{dx}{(h_1 - h_2)^3}\right). \tag{10}$$

The integrals in (10) will be independent of time only when L is an integral multiple of λ. In these problems either we have to prescribe Δp or $\bar{Q}$ and by prescribing either Δp or $\bar{Q}$ as constants, the flow can be treated as steady in wave frame. The integrals in (10) are evaluated over one wavelength using the values of the integrals given in Appendix and replacing q with $\bar{Q}$ from (8), we get

$$\begin{aligned}\Delta p &= -6\Big\{\bar{Q} - (1+d)\Big\}\frac{2(1+d)^2 + (a^2+b^2+2ab\cos\phi)}{\Big\{(1+d)^2 - (a^2+b^2+2ab\cos\phi)\Big\}^{5/2}} \\ &\quad - 12\frac{1+d}{\Big\{(1+d)^2 - (a^2+b^2+2ab\cos\phi)\Big\}^{3/2}},\end{aligned} \tag{11}$$

and this is rewritten in the form

$$\begin{aligned}\bar{Q} &= \frac{-\Delta p}{6}\frac{\Big\{(1+d)^2 - (a^2+b^2+2ab\cos\phi)\Big\}^{5/2}}{2(1+d)^2 + (a^2+b^2+2ab\cos\phi)} \\ &\quad + \frac{3(1+d)(a^2+b^2+2ab\cos\phi)}{2(1+d)^2 + (a^2+b^2+2ab\cos\phi)}.\end{aligned} \tag{12}$$

The results for the flow corresponding to a symmetric channel are obtained from our results by putting $a = b$, $d = 1$ and $\phi = 0$. Equation(12) reduces to Poiseuille law for a channel when $\Delta p < 0$; $a = b = 0$ channel with straight walls or $a = b$ and $\phi = \pi$ a channel with peristaltic waves with same amplitude and inphase.

3. Discussion of the results

3.1. Pumping Characterstics

The characterstic feature of peristaltic motion is pumping against pressure rise. From (12), we observe

$$\bar{Q} = 0 \text{ for } \Delta p = \Delta p_{max} = \frac{18(1+d)(a^2+b^2+2ab\cos\phi)}{\left\{(1+d)^2-(a^2+b^2+2ab\cos\phi)\right\}^{5/2}},$$

$$\text{and} \quad \bar{Q} = \bar{Q}_{max} = \frac{3(1+d)(a^2+b^2+2ab\cos\phi)}{2(1+d)^2+(a^2+b^2+2ab\cos\phi)},$$

for $\Delta p = 0$, (free pumping). When $\Delta p > \Delta p_{max}$ one gets negative flux and when $\Delta p < 0$, we get $\bar{Q} > \bar{Q}_{max}$ as the pressure assists the flow which is known as copumping. The complete occlusion (or the channel walls touch each other) occurs when $a^2+b^2+2ab\cos\phi = (1+d)^2$ and in that case the fluid is pumped as a positive displacement pump with $\bar{Q} = 1+d$.

The variation of time-average flux $\bar{Q}$ as a function $\phi/\pi = \bar{\phi}$, normalized phase difference, is calculated from equation (12) for different values of Δp and is presented in Fig. 2 for two different cases (i) when the amplitudes of the peristaltic wave on the upper and lower walls are same $a = b = 0.7$ and (ii) when the amplitudes are different $a = 0.7$, $b = 1.2$. From the curve for $\Delta p = 1.5$ in Fig. $2(i)$, we observe that when $\bar{\phi} = 0$, $\bar{Q}$ is maximum and decreases as $\bar{\phi}$ increases and becomes zero for some $\bar{\phi}$ and remains negative afterwards until $\bar{\phi}$ becomes 1. For $\Delta p > \Delta p_{max}$, even for $\bar{\phi} = 0$, $\bar{Q}$ becomes negative and remains so for all $0 < \bar{\phi} \leq 1$. When $\Delta p = 0$, for free pumping case, we observe $\bar{Q}$ is zero for $\bar{\phi} = 1$ (i.e when peristaltic waves are in phase, the cross section of the channel remains same through out) and is positive for all $0 \leq \bar{\phi} < 1$. $\bar{Q}$ remains always positive for $\Delta p < 0$ (i.e in the copumping range) as pressure assists the flow due to peristalsis on the walls. The positive rate of flux for $0 \leq \Delta p \leq \Delta p_{max}$ is entirely due to peristalsis. The results for same amplitude peristaltic waves with phase difference given by Eytan and Elad [3] agree with our results described above. When the amplitudes of the peristaltic waves are different, we observe for free pumping ($\Delta p = 0$), the rate of flux $\bar{Q}$ remains positive for all $0 \leq \bar{\phi} \leq 1$ as depicted in Fig. $2(ii)$. Here the positive flux is possible mainly because the different amplitude peristaltic waves on the walls produce an asymmetric channel of variable cross section. Further, it is easy to observe that the flux increases when the amplitudes (depend on d as given in (4)) of the pearistaltic waves increses. Fig. 3, depicts the variation of Δp with $\bar{Q}$ with $a = 0.7$, $b = 1.2$, $d = 2$ for different values of ϕ. An interesting observation here is that in copumping $\bar{Q}$ increases with ϕ, $0 \leq \phi \leq \pi$, for an appropriatly chosen $\Delta p(< 0)$ irrespective of the amplitudes being same or different.

The variation of flux $\bar{Q}$ with the width of the channel d, for fixed $a =$

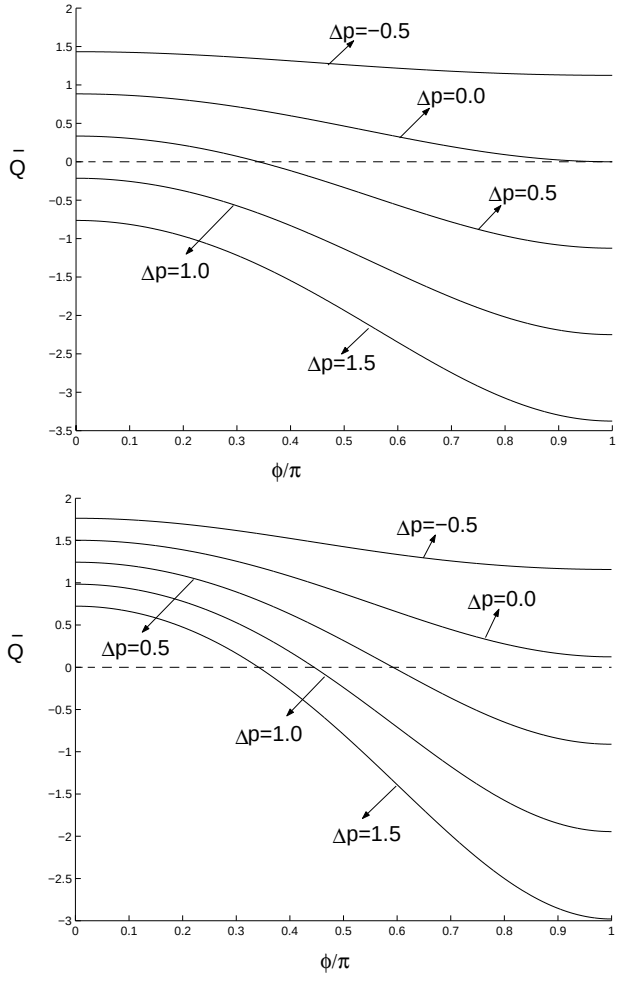

Figure 2. The variation $\bar{Q}$ with ϕ and d=2 for different values of Δp with (i) $a = 0.7,\ b = 0.7$, (ii) $a = 0.7,\ b = 1.2$.

$0.7,\ b = 1.2$ and $\phi = \pi/2$ is presented in Fig. 4 for different values of Δp. It is observed that for $\Delta p \geq 0$ the flux rate decreases as the distance d between the walls increases due to the reduction in the peristalsis effects. From the curve for $\Delta p = -0.05$ ($\Delta p < 0$ small) in Fig. 4, $\bar{Q}$ decreases for some d (small) in the beginning but it starts increasing for d large as the Poiseuille flow due to pressure loss dominates the peristaltic flow. Fig. 5 shows the variation of $\bar{Q}$ with one of the amplitudes b for fixed $a = 0.5,\ d = 1,\ \Delta p = 0.1$ for different values of ϕ. It shows that the rate of flux decreases and attains the minimum value at $b = -a\cos\phi$ and then it increases as b increases. Even when there is no wave on

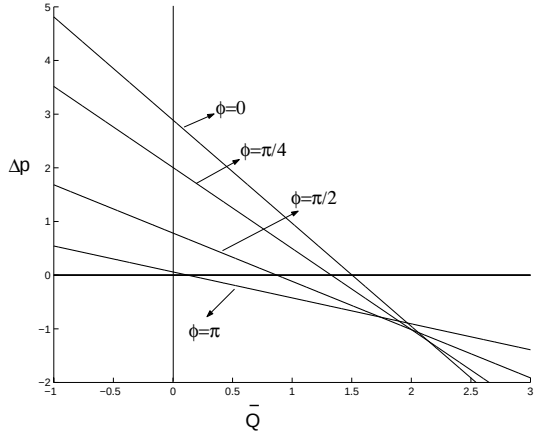

Figure 3. Variation of $\bar{Q}$ with Δp for different ϕ , and $a = 0.7,\ b = 1.2,\ d = 2.$.

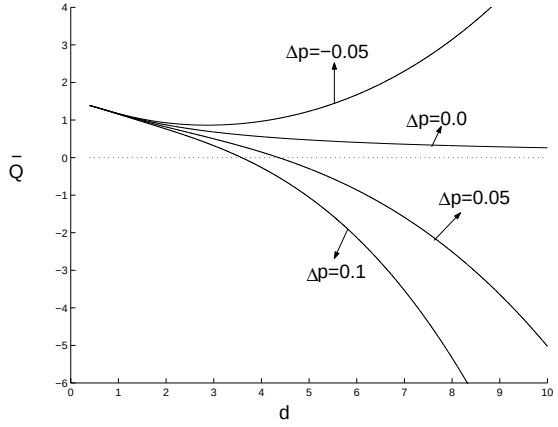

Figure 4. Variation of $\bar{Q}$ with d for different Δp with $a = 0.7,\ b = 1.2$ and $\phi = \pi/2$.

one of the walls i.e when $b = 0$, we observe that the flux rate is always positive.

3.2. Trapping

In the wave frame the streamlines in general have a shape similar to the walls as the walls are stationary. But under certain conditions some streamlines split (due to the existence of a stagnation point) to enclose a bolus of fluid particles in closed streamlines. In the fixed frame the bolus moves as a whole at the wave speed as if trapped by the wave. It is seen from the equation (7) that center streamline $(\psi = 0)$ is not only at $y = (h_1 + h_2)/2,$ but also on the curve defined by the

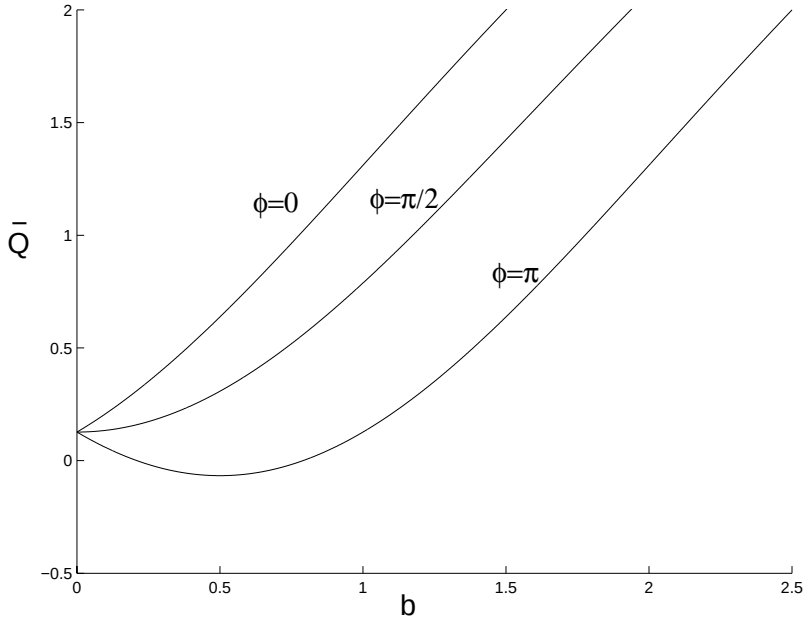

Figure 5. The variation of $\bar{Q}$ as a function of b with $a = 0.5, d = 1$ and $\Delta p = 0.1$ for different ϕ.

points given by

$$\begin{aligned} 2y^2\left\{(h_1-h_2)-(1+d)+\bar{Q}\right\}+2y\{h_1+dh_1-h_1^2+h_2+dh_2 \\ +h_2^2-h_1\bar{Q}-h_2\bar{Q}\}+\{h_1^2+dh_1^2-4h_1h_2-4dh_1h_2+2h_1^2h_2 \\ +h_2^2+dh_2^2-2h_1h_2^2-h_1^2\bar{Q}-h_2^2\bar{Q}+4h_1h_2\bar{Q}\}=0. \end{aligned} \tag{13}$$

Equation (13) gives two real roots for y, when the descriminent

$$\frac{-3(1+d)+(h_1-h_2)+3\bar{Q}}{h_1-h_2-1-d+\bar{Q}} \geq 0. \tag{14}$$

An analysis of the equation (13) shows that both the real roots lie with in the channel whenever $\bar{Q}$ satisfies the condition

$$\frac{2(1+d)-\sqrt{a^2+b^2+2ab\cos\phi}}{3} \leq \bar{Q} \leq \frac{2(1+d)+\sqrt{a^2+b^2+2ab\cos\phi}}{3}. \tag{15}$$

Equation (15) gives the upper and lower trapping limits on $\bar{Q}$ for the splitting of the center streamline.

The effect of phase shift ϕ on trapping with same amplitudes $a = b = 0.5$ for $\bar{Q} = 1.4$ (with in the centerline trapping limits) is illusrated in Fig. 6. It is observed that the bolus appearing in the center region for $\phi = 0$ moves towards left and decreases in size as ϕ increases. For $\phi = \pi$, the bolus dissapears and

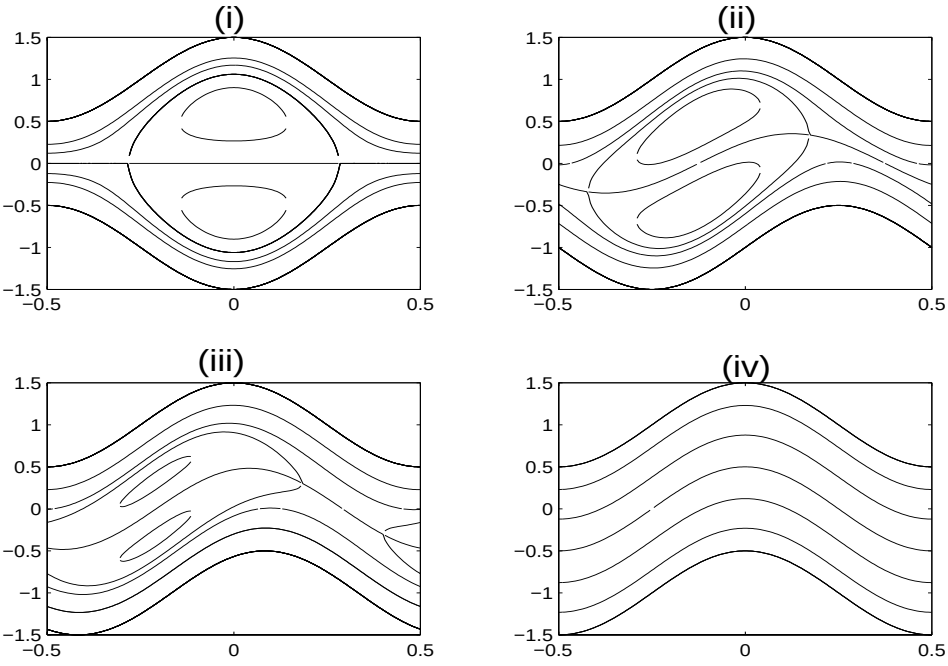

Figure 6. Streamlines for $a = 0.5,\ b = 0.5,\ d = 1,\ \bar{Q} = 1.4$ and for different ϕ $i)\phi = 0,\ \ ii)\phi = \frac{\pi}{2},\ \ iii)\phi = \frac{5\pi}{6},\ \ iv)\phi = \pi.$

the streamlines are parallel to the boundary walls (Pozrikidis [7]) and here $\bar{Q} > 0$ is possible only when $\Delta p < 0$ corresponding to Poiseuille flow. Fig. 7 gives the plots for $a = 0.3,\ b = 0.5$ (different amplitudes) and $\bar{Q} = 1.4$ at different values of ϕ and it shows that the trapping exists for all phase differences ϕ. Even when the walls are moving inphase, $(\phi = \pi)$ with different amplitudes trapping exists due to non zero flux rate $\bar{Q}$. For fixed $\bar{Q}$, Δp $(> 0$ for $\phi = 0)$ decreases as ϕ increases and may become negative for $\phi = \pi$ and corresponding the trapping region decreases as seen from Fig. 6 and Fig. 7. Streamlines with same as well as different amplitudes with different phases in a fixed frame of reference are shown in Fig. 8 and these agree with the streamline patterns shown by Pozrikidis [7].

It is observed when the flux lies between $\bar{Q}_{max} < \bar{Q} < 1+d$ a streamline other than $\psi = 0$ splits and the results of trapping near the centerline are shown in Fig. 9(i) and (ii). When $\bar{Q} > 1 + d$, in the copumping region, the trapping moves towards the boundary walls and its size reduces as $\bar{Q}$ increases as depicted in Fig. 9(iii) and (iv). The values of the parameters chosen are given in the captions. Similar type of phenomena was observed in copumping zone by Ramachandra Rao and Usha [8] in the study of peristaltic transport in two fluid system. When either a or b equals to zero, peristaltic wave exists only on one of the walls,

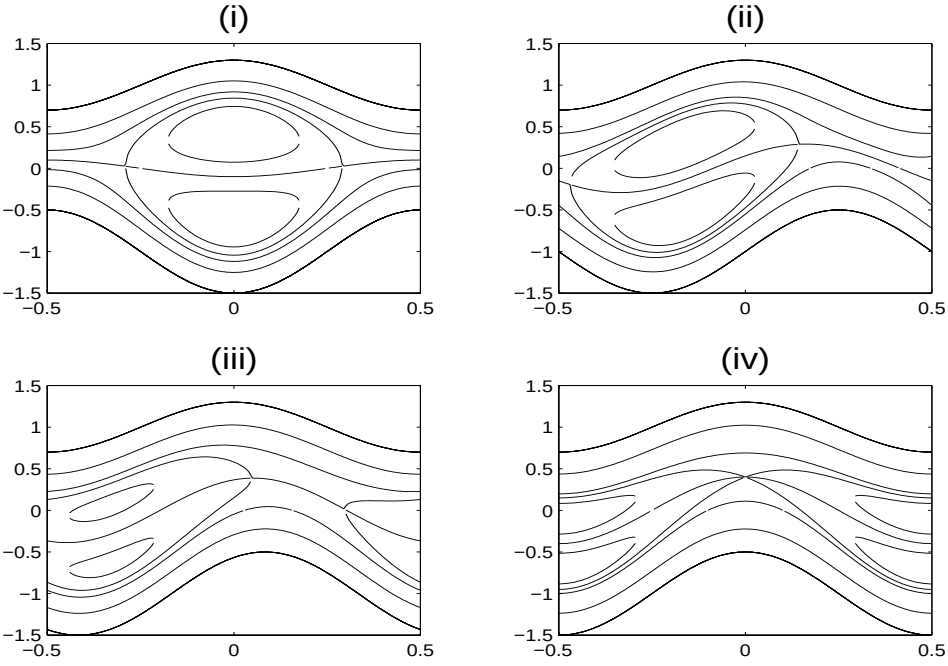

Figure 7. Streamlines for $a = 0.3,\ b = 0.5,\ d = 1,\ \bar{Q} = 1.4$ and for different ϕ $i)\phi = 0,\ \ ii)\phi = \frac{\pi}{2},\ \ iii)\phi = \frac{5\pi}{6},\ \ iv)\phi = \pi.$

the mechanism of trapping remains the same and the trapping phenomena at the centerline and near the boundary of the channel are shown in Fig. 10.

Fig. 11 illustrates the effect of the width of the channel for a fixed $\bar{Q} = 1.4,\ \phi = \pi/2,\ a = b = 0.5$ for different values of d. The trapping occuring for small d (Fig. $11(i)$) near the boundary (as $\bar{Q} = 1.4$ falls in the copuming range) moves to the center line(with the existence of stagnation point, $\bar{Q}$ lies in the trapping limits given in (15))for $d = 1.0$ (Fig. $11(ii)$) and disappears for large d ($\bar{Q}$ lies outside the trapping limits) see Fig. 10 (iii), and (iv). From Fig. 11, we conclude for a given $\bar{Q}$, one can find the width of the channel for which trapping occurs near the boundary, centerline or no where.

3.3. Reflux

Reflux is defined as the presence of some fluid particles whose mean motion over one cycle is against the net pumping direction. Following Shapiro *et al.* [9], Q_ψ defined as dimensionless volume flow rate in the fixed frame between the centerline of the channel $(h_1 + h_2)/2$ and the wave frame streamline ψ, which

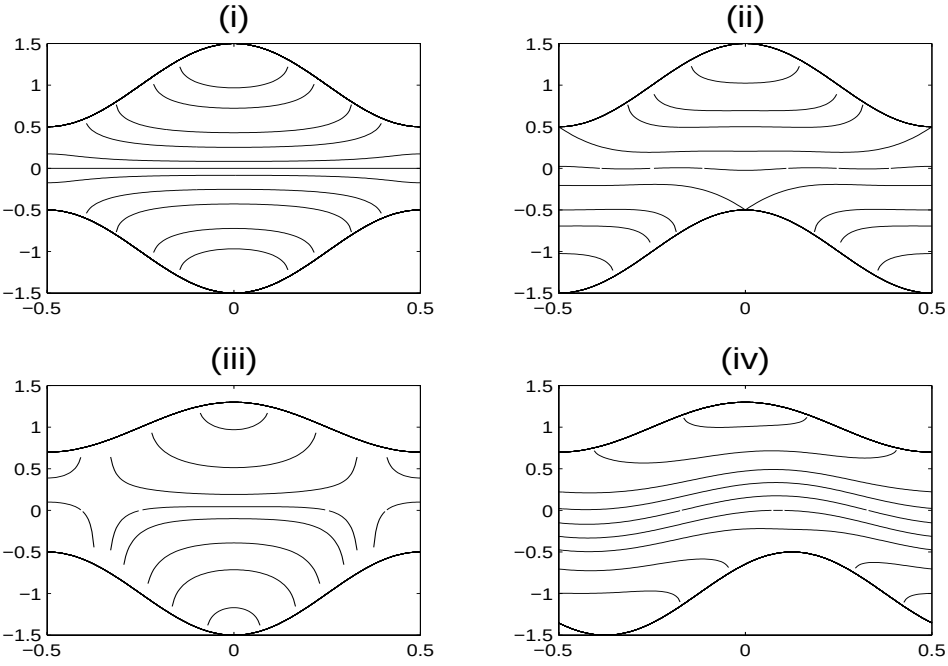

Figure 8. Streamlines in a fixed frame of reference with $d = 1$ $(i)a = b = 0.5,\ \bar{Q} = 1.4,\ \phi = 0,\ (ii)a = b = 0.5,\ \bar{Q} = 1.4,\ \phi = \pi, (iii)a = 0.3,\ b = 0.5,\ \bar{Q} = 0.5,\ \phi = 0,$ and $(iv)a = 0.3,\ b = 0.5,\ \bar{Q} = 2.5,\ \phi = \frac{3\pi}{4}$

is an indicator of material particles in fixed frame, and is given by

$$Q_\psi = \int_{(h_1+h_2)/2}^{Y(\psi,X,t)} U(X,Y,t)dY. \tag{16}$$

By using the transformation between the two frames given in equation (2) and integrating (16), we get

$$Q_\psi = \psi + y(\psi, X, t) - \frac{h_1 + h_2}{2}. \tag{17}$$

Averaging (17) over one period of the wave, we get

$$\bar{Q}_\psi = \psi + \int_0^1 y(\psi, x)dx - \frac{1-d}{2} \tag{18}$$

Now define $Q^* = \bar{Q}_\psi/\bar{Q}_w,\ \ \psi^* = \psi/\psi_w,$ where $\bar{Q}_w$ and ψ_w are the values of $\bar{Q}_\psi$ and ψ at the wall, at $y = h_1,\ \bar{Q}_w = \bar{Q}/2$ and $\psi_w = (\bar{Q} - 1 - d)/2$. According to Shapiro *et al.* [9] reflux layer exists near the wall, whenever Q^* increases to a value greater than one and decreases to one at the wall.

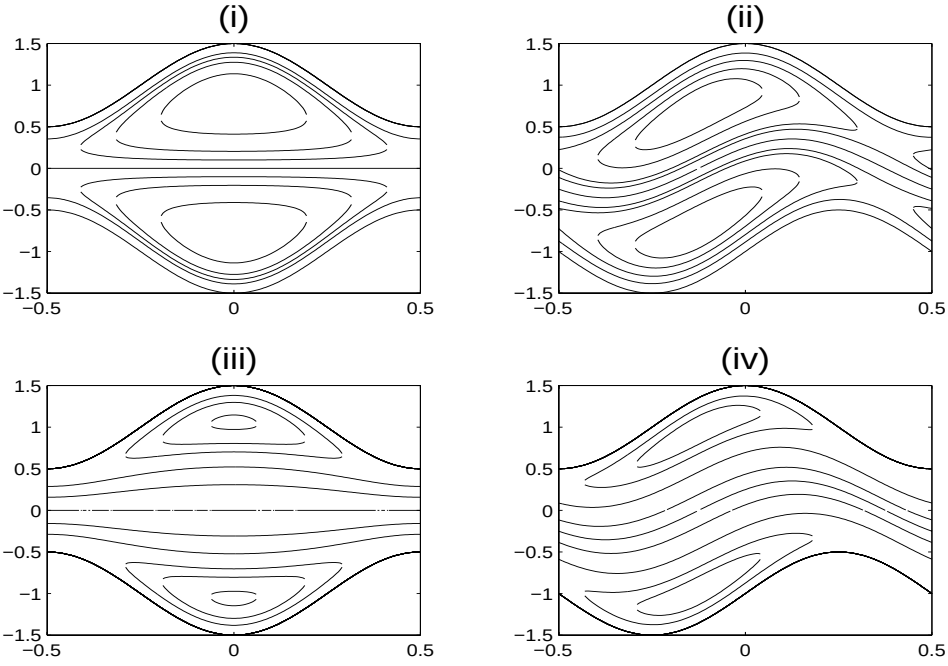

Figure 9. Streamlines for $a = 0.5,\ b = 0.5,$ and $d = 1$ with $\bar{Q} = 1.8$ (pumping region) $(i)\phi = 0,\ (ii)\phi = \pi/2$ and $\bar{Q} = 3.0$ (copumping region) $(iii)\phi = 0\ (iv)\phi = \frac{\pi}{2}$.

The integrand of (18) is found by solving (7), a cubic, for y as a function of x. The integral is evaluated by using a numerical quadrature. Fig. $12(i)$ shows the variation of Q^* as a function of ψ^* for a fixed value of $\bar{Q}_w = 0.05$, lying in the reflux zone (given by equation (21) later) and $a = b = 0.5,\ d = 1$. If Q^* increases with an increase in ψ^* then the motion of the particles is always in the pumping direction and reflux appears where Q^* decreases with increasing ψ^*. From Fig $12(i)$, it is clearly seen that curve for $\phi = 0$ (corresponding to the symmetric channel) reflux exists near the boundary wall. We observe, as ϕ increases the reflux zone reduces and it is actually absent when $\phi = 3\pi/4$ and π as seen from the Fig. $12(i)$. It appears that reflux zone present in a symmetric channel may disappear when the channel becomes asymmetric through the phase difference of the peristaltic waves on the walls as expected from the pumping characterstics. These results agree with the evaluation of particle trajectories given by Eytan and Elad [3]. The variation of Q^* with ψ^* for the case with $a = 0.5,\ b = 0.2,\ \bar{Q} = 0.02$ is depicted in Fig. $12\,(ii)$. The interesting phenomena observed here is, a reflux zone exists near the boundary wall even for $\phi = \pi$, as positive pumping is possible in a variable cross section channel. We observe that the reflux zones are bigger for all ϕ in Fig. $12\,(ii)$ compared with Fig. $12(i)$

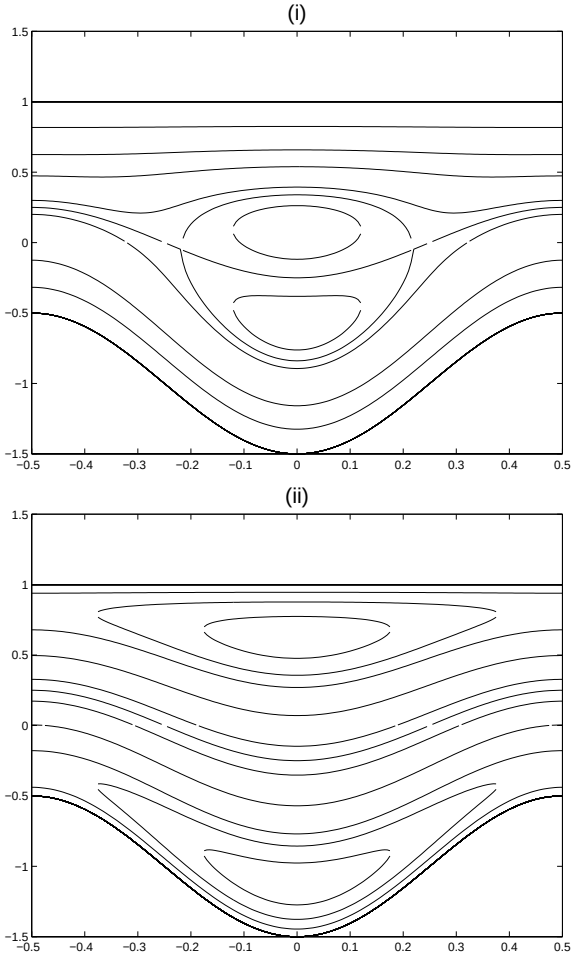

Figure 10. Streamlines for wave at one wall i.e. $a = 0.0,\ b = 0.5$ and $d = 1,$ for $(i)\ \bar{Q} = 1.3$ (pumping region) and $(ii)\ \bar{Q} = 2.8$ (copuming region).

for the cases considered. It appears that $\bar{Q}$ small leads to bigger reflux zones in general. The effects of channel width on reflux layer is illustrated in Fig. 13 and it is observed that the reflux layer decreases with an increase in d and completely absent for d large.

In order to obtain the limits on $\bar{Q}$ for reflux, we expand y about the wall in powers of a small parameter ϵ, where

$$\epsilon = \psi - \psi_{y=h_1} = \psi + \frac{1 + d - \bar{Q}}{2},$$

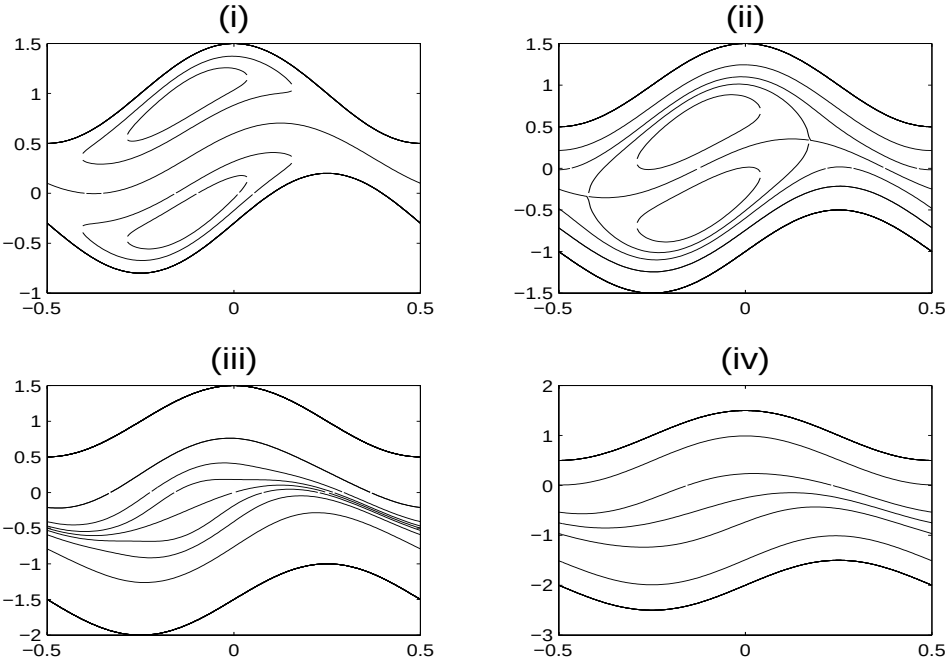

Figure 11. Streamlines for $a = b = 0.5,\ \phi = \pi/2,\ \bar{Q} = 1.4$ with varying channel width d $(i)\ d = 0.3\ (ii)\ d = 1.0\ (iii)\ d = 1.5,\ (iv)\ d = 2$

and we get

$$y = h_1 - \epsilon - \frac{3\epsilon^2}{h_1 + h_2}\Big\{\frac{\bar{Q} - (1+d)}{h_1 - h_2} + 1\Big\} + \cdots . \tag{19}$$

Using (19) in the integral (18), one gets

$$\bar{Q}_\psi = \frac{\bar{Q}}{2} - 3\epsilon^2\Big\{\frac{\bar{Q}(1+d) - (a^2 + b^2 + 2ab\cos\phi}{\Big\{(1+d)^2 - (a^2 + b^2 + 2ab\cos\phi)\Big\}^{3/2}}\Big\} + \cdots . \tag{20}$$

Applying the reflux condition $Q^* = \bar{Q}_\psi/\bar{Q}_w > 1$, one obtains the reflux limit as

$$\bar{Q} < \frac{a^2 + b^2 + 2ab\cos\phi}{1+d}. \tag{21}$$

By putting $a = b,\ d = 1$ in (21), we obtain the reflux limit for a symmetric channel which agrees with the results existing in the literature. Similar results can be obtained near the other boundary wall $y = h_2$.

Fig. 14 shows the trapping and reflux limits by the variation of $\bar{Q}/\bar{Q}_{max}$ with $a = b = \kappa$ and $d = 1$ for different ϕ. The region of trapping is more for a symmetric channel. This is consistent with the earlier results shown in Figs. 6

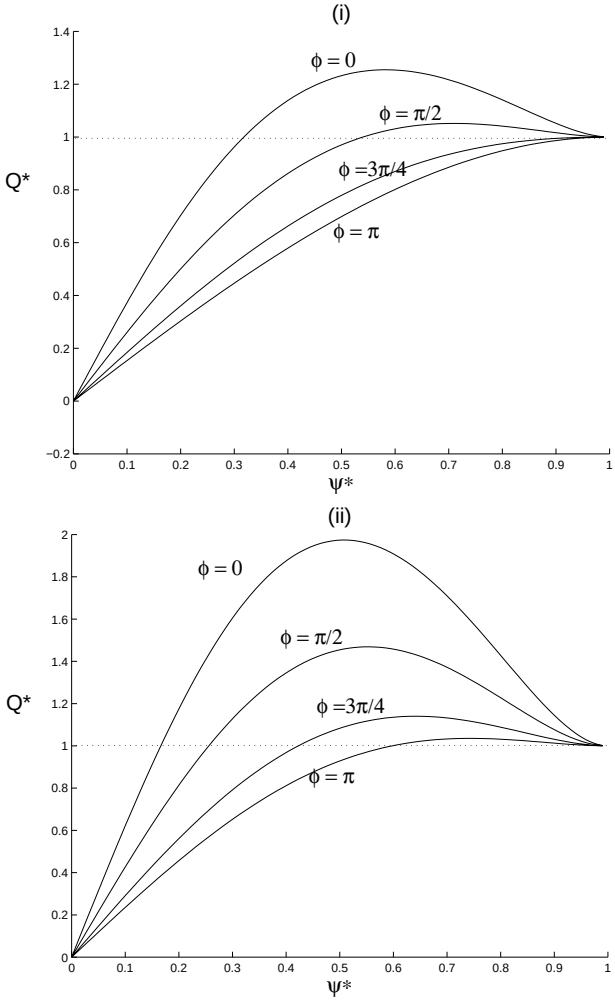

Figure 12. Q^* versus ψ^* for different ϕ with fixed
$(i)\ \bar{Q} = 0.1,\ a = b = 0.5,\ d = 1,\ (ii)\ \bar{Q} = 0.02,\ a = 0.5,\ b = 0.2,\ d = 1.$

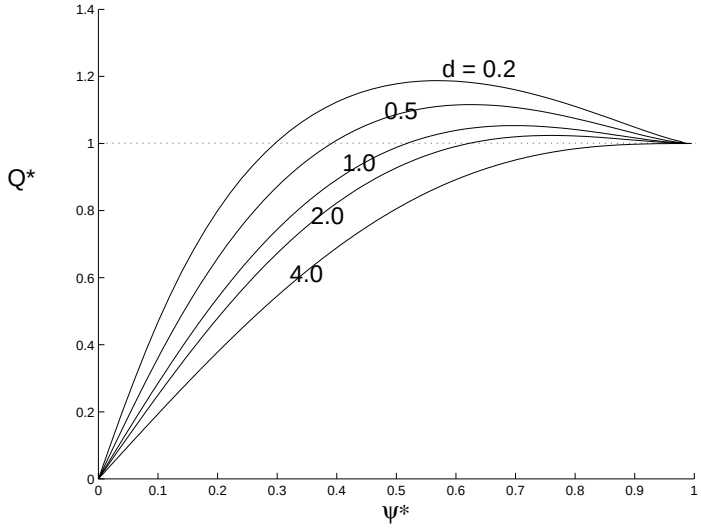

Figure 13. Q^* versus ψ^* for different d with fixed $\bar{Q} = 0.2$, $a = b = 0.5$, and $\phi = 0$

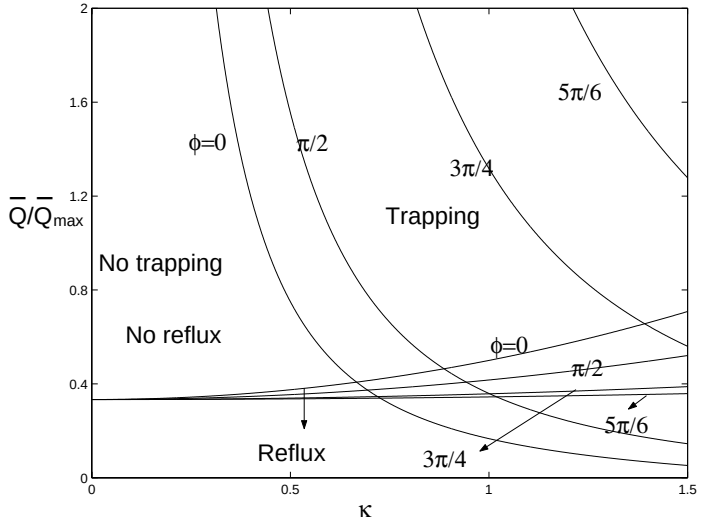

Figure 14. Trapping and reflux limit for different ϕ with $d = 1$

and 7. It is also observed that the reflux layer decreases with an increasing ϕ conforming the results shown in Fig. 12. Similar results for reflux and trapping can be obtained for the case of an asymmetric channel.

4. Conclusions

A mathematical model to study the peristaltic transport of a newtonian fluid in a genaralised asymmetric channel, under the assumptions of low Reynolds number and small curvature is presented. The important fluid mechanics phenomena of peristaltic transport, the pumping characteristics such as the reflux, the trapping and the variation of time-averaged flux with pressure rise as function of the asymmetric motility parameters, is discussed with the help of a simple analytical solution. The method followed here is different from earlier methods due to Eytan and Elad [3] and Pozrikidis [7]. The results obtained by us agree with their results. More effects due to asymmetry arising through different amplitudes and phase are studied with ease through our analysis. Symmetric channel gives more rate of flux and bigger trapping zone and reflux layer than the asymmetric channel. The results given here may throw some light on the fluid dynamic aspects of the intra-uterine fluid flow induced by uterine contractions studied by Eytan and Elad [3]. For a more realistic model of intra-uterine fluid flows one may have to model the sagittal cross section of the uterus by a tapering channel and the uterine fluid by an appropriate non-Newtonian fluid.

Appendix

$$\int_0^{2\pi} \frac{d\theta}{\alpha + \beta\cos\theta + \gamma\sin\theta} = \frac{2\pi}{\sqrt{\alpha^2 - \beta^2 - \gamma^2}}, \qquad \alpha > \sqrt{\beta^2 + \gamma^2} \tag{A1}$$

$$\int_0^{2\pi} \frac{d\theta}{(\alpha + \beta\cos\theta + \gamma\sin\theta)^2} = \frac{2\pi\alpha}{(\alpha^2 - \beta^2 - \gamma^2)^{3/2}} \tag{A2}$$

$$\int_0^{2\pi} \frac{d\theta}{(\alpha + \beta\cos\theta + \gamma\sin\theta)^3} = \frac{\pi(2\alpha^2 + \beta^2 + \gamma^2)}{(\alpha^2 - \beta^2 - \gamma^2)^{5/2}} \tag{A3}$$

Integral $(A1)$ is evaluated by contour integration, $(A2)$ and $(A3)$ are obtained by parametric differentiation from $(A1)$.

Acknowledgements

The author M. Mishra would like to thank Dr. S. Usha for the valuable discussions on the computational aspects of this work.

References

[1] S. Boyarsky, Surgical physiology of the renal pelvis, *Monogr. Surg. Sci.* **1** (1964), 173-213.
[2] K. De Vries, E. A. Lyons, J. Ballard, C. S. Levi, and D. J. Lindsay, Contractions of the inner third of the myometrium, *Am. J. Obstetrics Gynecol.* **162**(1990), 679-682.
[3] O. Eytan, and D. Elad, Analysis of Intra-Uterine fluid motion induced by uterine contractions, *Bull. Math. Biology* **61** (1999), 221-238.
[4] O. Eytan, A. J. Jaffa, J. Har-Toov, E. Dalach, and D. Elad, Dynamics of the intrauterine fluid-wall interface, *Annals of Biomedical eng.* **27** (1999), 372-379.
[5] Y.C. Fung and C. S. Yih, Peristaltic transport. *J. Appl. Mech.* **35** (1968), 669-675.
[6] F. Kill, *The function of the ureter and the renal pelvis*. Saunders: Philadelphia (1957).
[7] C Pozrikidis, A study of peristaltic flow, *J. Fluid Mech.* **180** (1987), 515-527.
[8] A. Ramachandra Rao, and S. Usha, Peristaltic transport of two immiscible viscous fluid in a circular tube, *J. Fluid Mech.* **298** (1995), 271-285.
[9] A. H. Shapiro, M. Y. Jaffrin, and S. L. Weinberg, Peristaltic pumping with long wavelengths at low Reynlods number, *J. Fluid Mech.* **37** (1969), 799-825.
[10] J. B. Shukla and S. P. Gupta, Peristaltic transport of a powerlaw fluid with variable consistency, *J. Biomech. Eng.* **104** (1982), 182-186.
[11] L. M. Srivastava, and V. P. Srivastava, Peristaltic transport of blood: Casson model II, *J. Biomech.* **17** (1984), 821-829.
[12] S. Takabatake, and K. Ayukawa, Numerical study of two-dimensional peristaltic flow, *J.Fluid Mech.* **122** (1982), 439-465.
[13] S. L. Weinberg, E. C. Eckistein, and A. H. Shapiro, An experimental study of peristaltic pumping, *J. Fluid Mech.* **49**(1971), 461-497.
[14] C. C. Yin and Y. C. Fung, Peristaltic waves in circular cylindrical tubes, *J. Appl. Mech.* **36** (1969), 579-587.
[15] C. C. Yin and Y. C. Fung, Comparison of theory and experiment in peristaltic transport, *J. Fluid Mech.* **47** (1971), 93-112.

Manoranjan Mishra and Adabala Ramachandra Rao
Department of Mathematics
Indian Institute of Science
Bangalore-560012
India
e-mail: ramachand@math.iisc.ernet.in

(Received: May 18, 2001; revised: November 11, 2001)